

THE SECOND VS. THE THIRD MOMENT MATCHING BETWEEN DIFFUSION MODELS FOR DYNAMIC ADSORBER

Dong-Ik Song

Department of Chemical Engineering, Kyungpook National University,
1370 Sangyuk dong, Pook ku, Taegu 702-701, Korea
(Received 8 June 1995 • accepted 6 September 1995)

Abstract—Four diffusion models for the dynamic adsorber, i.e. LDF model, single diffusivity diffusion model, two diffusivity diffusion model for beds packed with bidisperse and/or zeolite-type particles, were considered. The third moments for the four diffusion models were obtained. Relations between the system parameters involved in each model were derived by matching mean, variance or the third moment between diffusion models. The two relations from either variance or the third moment matching were examined to investigate which one is superior when model simplification is required, by comparing the time domain elution curves for the single and the two diffusivity diffusion models. For the symmetric elution curves, relation from the variance matching is much better as expected, than the relation matching the third moment which measures skewness about mean. As the elution curves become highly asymmetric, eluting shortly after injection and exhibiting long tailing due to both the small intraparticle diffusivities and small space time in the adsorber, either relation failed to satisfactorily simplify the two diffusivity diffusion model. Contrary to the expectation that the third moment matching would work better in the asymmetric curves due to the nature of the third moment, variance matching still gives slightly better results. Relation from the variance, instead of the third moment, matching is strongly recommended for model simplification due to its simplicity in formula.

Key words: Adsorber, Variance, Third Moment, Effective Diffusivity, Macropore Diffusivity, Micropore Diffusivity

INTRODUCTION

Particles with bidisperse pore structure are widely used as heterogeneous catalysts, adsorbents for separation and purification etc. in several processes of chemical industry. Since reaction rate inside the commercial catalysts is usually very high, the overall reaction rate is controlled mostly by the intraparticle diffusion process like in most separation processes using adsorbent. Models for the dynamic adsorber packed with either monodisperse or bidisperse particles are usually described using the system parameters such as the adsorption rate and equilibrium constants assuming a finite linear reversible rate of adsorption, external film mass transfer coefficient and axial dispersion coefficient, in addition to the respective intraparticle effective diffusivities. For beds packed with bidisperse particles, besides the interparticle mass balance, two additional intraparticle diffusion equations for the particle and the microparticle are required to realistically describe the intraparticle diffusion processes, using the macro- and micropore effective diffusivities respectively. Diffusion equation for the microcrystal is sometimes replaced with the single phase solid diffusion equation for beds packed zeolite-type particles in particular. However, if one regards the bidisperse particles as monodisperse, only one intraparticle diffusion equation is needed using a single effective diffusivity. In view of the computational convenience achieved by eliminating one diffusion equation for the microparticle, the single effective diffusivity model is more attractive than the two effective diffusivity one.

In linear driving force (LDF) diffusion model [Glueckauf and Coates], all the mass transfer processes except for the axial dis-

persion are lumped into a linear transport rate expression using an overall effective mass transfer coefficient, thus completely eliminating mass balance equation for the adsorbing particle. Raghavan and Ruthven [1985] have shown that the effective overall mass transfer coefficient in the LDF model is related to the various system parameters by matching variances from both LDF and diffusion models for a bed packed with bidisperse particles. In extension of this work, Kim [1990] has obtained the relationship between the single effective diffusivity and the macro- and micropore effective diffusivities by means of the matching of the variances from both the single and the two diffusivity diffusion models. Kim [1990] examined the adequacy of the relation by directly comparing the time domain solutions of the two diffusion models, and revealed that its performance becomes poor as both the space time and the two effective diffusivities are simultaneously small, leading to the highly asymmetric elution curves. This point is well expected since the relation is derived by matching variances, not the third moments representing skewness about the mean, from the two diffusion models. Hsu and Haynes [1981] addressed that much information for the response curve is lost when only mean and variance are used in determining system parameters due to the difficulties involved in computing higher moments from the experimental response curves.

In view of these points, the degree of asymmetry about the mean which is associated with the third central moment is considered in this work to see if the new relationship from the matching of the third moment instead of variance gives better agreement in the time domain solutions especially in the highly asymmetric response curves. In the present work, the third central moment will be computed for the first time for the LDF, single and two diffusivity, and zeolite-type diffusion models considering

†To whom all correspondences should be addressed.

all the possible mass transfer resistances for completeness, and the new relation among the system parameters involved in various diffusion models will be derived from the mean, variance, or third moment matching. Each relation obtained via matching will be examined in the time domain by numerically inverting the Laplace transformed solutions for the single and the two diffusivity diffusion models.

DIFFUSION MODELS

1. LDF Model

Linear driving force (LDF) diffusion model [Glueckauf-Coates, 1947] for the dynamic adsorber has been widely used for its simplicity and ease of computation. In this model, all the diffusion processes except the dispersion due to the bulk convective motion were modeled as a linear mass transfer rate to eliminate mass balance for the adsorbing particle.

$$\frac{\partial \bar{Q}_p}{\partial t} = k[C(z, t) - C^*(z, t)] \tag{1}$$

where \bar{Q}_p is the particle volume averaged total adsorbate concentration, C the adsorbate concentration in the mobile fluid and C^* the mobile phase concentration in equilibrium with the volume averaged adsorbed phase concentration \bar{Q}_p . Hence, assuming linear adsorption for the very small adsorbate concentration in the mobile fluid,

$$\bar{Q}_p(z, t) = K \cdot C^* \tag{2}$$

where K represents a pseudoadsorption equilibrium constant modified for the total adsorbate concentration instead of the adsorbed phase concentration. Mass balance for the adsorbate in the mobile fluid phase is,

$$\frac{\partial C}{\partial t} = \frac{D_z}{\epsilon} \frac{\partial^2 C}{\partial z^2} - v \frac{\partial C}{\partial z} - \frac{1-\epsilon}{\epsilon} \frac{\partial \bar{Q}_p}{\partial t} \tag{3}$$

Initial and boundary conditions are

$$C(z, 0) = 0, \bar{Q}_p(z, 0) = 0, C(0, t) = \delta(t), C(\infty, t) = 0 \tag{4}$$

The n -th absolute moment, μ_n' can be obtained either from the derivatives of the Laplace transformed solution $\bar{C}(L, s)$ for the mathematical model or from the integration of the time domain solution, $C(L, t)$ as follows.

$$\mu_n' = (-1)^n \lim_{s \rightarrow 0} \frac{d^n \bar{C}(L, s)}{ds^n} = \int_0^\infty t^n \cdot C(L, t) dt \tag{5}$$

The first absolute and second central moments for the LDF model were already obtained by many researchers [Ruthven, 1984; Raghavan and Ruthven, 1985]. The first absolute moment, or mean, is

$$\mu_1' = \int_0^\infty t \cdot C(L, t) dt = \frac{L}{v} (1 + \delta_1) \tag{6}$$

where

$$\delta_1 = \frac{1-\epsilon}{\epsilon} K \tag{7}$$

The second central moment, or the variance, is

$$\mu_2 = \int_0^\infty (t - \mu_1')^2 \cdot C(L, t) dt = \mu_2' - (\mu_1')^2$$

$$= 2 \frac{L}{v} \left[\frac{D_z}{\epsilon} \frac{(1 + \delta_1)^2}{v^2} + \frac{1-\epsilon}{\epsilon} \frac{K^2}{k} \right] \tag{8}$$

The third central moment which is known to be a measure of the symmetry with respect to the mean is obtained as follows.

$$\begin{aligned} \mu_3 &= \int_0^\infty (t - \mu_1')^3 \cdot C(L, t) dt = \mu_3' - 3\mu_1' \mu_2' + (\mu_1')^3 \\ &= 6 \frac{L}{v} \left[2 \frac{D_z}{\epsilon} \frac{1 + \delta_1}{v^2} \left\{ \frac{D_z}{\epsilon} \frac{(1 + \delta_1)^2}{v^2} + \frac{1-\epsilon}{\epsilon} \frac{K^2}{k} \right\} + \frac{1-\epsilon}{\epsilon} \frac{K^3}{k^2} \right] \end{aligned} \tag{9}$$

2. Single Diffusivity Diffusion Model

Packed bed diffusion model for the single effective diffusivity has been formulated by Schneider and Smith [1968], considering all the possible transport rate processes such as the axial dispersion in the bed, external film mass transfer, and intraparticle diffusion, as well as the finite adsorption rate inside the particle. Mass balances for the adsorbable solute in the mobile fluid and stationary fluid inside the particles are respectively

$$\frac{\partial C_1}{\partial t} = \frac{D_z}{\epsilon} \frac{\partial^2 C_1}{\partial z^2} - v \frac{\partial C_1}{\partial z} - \frac{3}{R_p} \frac{1-\epsilon}{\epsilon} D_p \frac{\partial C_p}{\partial R} \Big|_{R=R_p} \tag{10}$$

$$\frac{\partial C_p}{\partial t} = \frac{D_p}{\epsilon_p} \frac{1}{R^2} \frac{\partial}{\partial R} \left(R^2 \frac{\partial C_p}{\partial R} \right) - \frac{1}{\epsilon_p} \frac{\partial Q}{\partial t} \tag{11}$$

The adsorption rate was assumed to be linear due to the very small solute concentration in the particle.

$$\frac{\partial Q}{\partial t} = k_a \left[C_p(z, R, t) - \frac{Q(z, R, t)}{K_a} \right] \tag{12}$$

where the adsorbed phase concentration, Q is based upon the volume of the particle. Initial and boundary conditions are,

$$C_1(z, 0) = 0, C_p(z, R, 0) = 0, Q(z, R, 0) = 0 \tag{13}$$

$$C_1(0, t) = \delta(t), C_1(\infty, t) = 0 \tag{14}$$

where $\delta(t)$ denotes unit impulse at the bed inlet.

$$D_p \frac{\partial C_p}{\partial R} \Big|_{R=R_p} = k_f [C_1(z, t) - C_p(z, R_p, t)], \frac{\partial C_p}{\partial R} \Big|_{R=0} = 0 \tag{15}$$

The first absolute and second central moments for the above mathematical model were obtained by Schneider and Smith [1968]. The first absolute moment and the second central moment are

$$\mu_1' = \frac{L}{v} (1 + \delta_1) \tag{16}$$

$$\mu_2 = 2 \frac{L}{v} \left[\frac{D_z}{\epsilon} \frac{(1 + \delta_1)^2}{v^2} + \delta_p \right] \tag{17}$$

where

$$\delta_1 = \frac{1-\epsilon}{\epsilon} (\epsilon_p + K_a) \tag{18}$$

$$\delta_p = \frac{1-\epsilon}{\epsilon} \left[\frac{K_a^2}{k_a} + (\epsilon_p + K_a)^2 \left(\frac{1}{15} \frac{R_p^2}{D_p} + \frac{1}{3} \frac{R_p}{k_f} \right) \right] \tag{19}$$

The third central moment is computed as

$$\mu_3 = 6 \frac{L}{v} \left[2 \frac{D_z}{\epsilon} \frac{1 + \delta_1}{v^2} \left\{ \frac{D_z}{\epsilon} \frac{(1 + \delta_1)^2}{v^2} + \delta_p \right\} + \delta_3 \right] \tag{20}$$

where

$$\begin{aligned} \delta_3 = & 2\delta_1 \frac{K_a^2}{k_a} \left(\frac{1}{15} \frac{R_p^2}{D_p} + \frac{1}{3} \frac{R_p}{k_f} \right) \\ & + \frac{1-\varepsilon}{\varepsilon} \left[\frac{K_a^3}{k_a^2} + \frac{(\varepsilon_p + K_a)^3}{315} \left\{ 35 \left(\frac{R_p}{k_f} \right)^2 \right. \right. \\ & \left. \left. + 14 \left(\frac{R_p^2}{D_p} \right) \left(\frac{R_p}{k_f} \right) + 2 \left(\frac{R_p^2}{D_p} \right)^2 \right\} \right] \end{aligned} \quad (21)$$

3. Two Diffusivity Diffusion Model

Mass balances for the small adsorbable component in the beds packed with bidisperse particles were formulated by Hashimoto and Smith [1973], considering a finite rate of adsorption. Mass balance in the mobile fluid is

$$\frac{\partial C_2}{\partial t} = \frac{D_z}{\varepsilon} \frac{\partial^2 C_2}{\partial z^2} - v \frac{\partial C_2}{\partial z} - \frac{3}{R_p} \frac{1-\varepsilon}{\varepsilon} D_a \frac{\partial C_a}{\partial R} \Big|_{R=R_p} \quad (22)$$

Mass balance equations in the stationary macropore and micropore fluids are respectively

$$\frac{\partial C_a}{\partial t} = \frac{D_a}{\varepsilon_a} \frac{1}{R^2} \frac{\partial}{\partial R} \left(R^2 \frac{\partial C_a}{\partial R} \right) - \frac{3}{r_c} \frac{1-\varepsilon_a - \varepsilon_b}{\varepsilon_a} D_i \frac{\partial C_i}{\partial r} \Big|_{r=r_c} \quad (23)$$

$$\frac{\partial C_i}{\partial t} = \frac{1-\varepsilon_a - \varepsilon_b}{\varepsilon_i} \frac{D_i}{r^2} \frac{\partial}{\partial r} \left(r^2 \frac{\partial C_i}{\partial r} \right) - \frac{1}{\varepsilon_i} \frac{\partial Q}{\partial t} \quad (24)$$

where

$$\frac{\partial Q}{\partial t} = k_a \left[C_i(z, R, r, t) - \frac{Q(z, R, r, t)}{K_a} \right] \quad (25)$$

In the above formulation, adsorption was assumed to occur in the micropores only due to the much higher adsorbable surface area in the micropores compared with that in the macropores, and the size of the microparticles was assumed to be uniform for conciseness. Initial and boundary conditions are,

$$\begin{aligned} C_2(z, 0) = 0, \quad C_a(z, R, 0) = 0, \quad C_i(z, R, r, 0) = 0, \\ Q(z, R, r, 0) = 0 \end{aligned} \quad (26)$$

$$C_2(0, t) = \delta(t), \quad C_2(\infty, t) = 0 \quad (27)$$

$$D_a \frac{\partial C_a}{\partial R} \Big|_{R=R_p} = k_f [C_2(z, t) - C_a(z, R_p, t)], \quad \frac{\partial C_a}{\partial R} \Big|_{R=0} = 0 \quad (28)$$

$$C_i(z, R, r_c, t) = C_a(z, R, t), \quad \frac{\partial C_i}{\partial r} \Big|_{r=0} = 0 \quad (29)$$

The first absolute and the second central moments for this model were obtained by Hashimoto and Smith [1973], and are shown below respectively.

$$\mu_1' = \frac{L}{v} (1 + \delta_1) \quad (30)$$

$$\mu_2 = 2 \frac{L}{v} \left[\frac{D_z}{\varepsilon} \frac{(1 + \delta_1)^2}{v^2} + \delta_a + \delta_b \right] \quad (31)$$

where

$$\delta_1 = \frac{1-\varepsilon}{\varepsilon} (\varepsilon_a + \varepsilon_i + K_a) \quad (32)$$

$$\delta_a = \frac{1-\varepsilon}{\varepsilon} (\varepsilon_a + \varepsilon_i + K_a)^2 \left(\frac{1}{15} \frac{R_p^2}{D_a} + \frac{1}{3} \frac{R_p}{k_f} \right) \quad (33)$$

$$\delta_b = \frac{1-\varepsilon}{\varepsilon} \left[\frac{K_a^2}{k_a} + \frac{1}{15} \frac{(\varepsilon_i + K_a)^2}{1-\varepsilon_a - \varepsilon_b} \left(\frac{r_c^2}{D_i} \right) \right] \quad (34)$$

The newly obtained third central moment is written as follows.

$$\mu_3 = 6 \frac{L}{v} \left[2 \frac{D_z}{\varepsilon} \frac{1 + \delta_1}{v^2} \left\{ \frac{D_z}{\varepsilon} \frac{(1 + \delta_1)^2}{v^2} + \delta_a + \delta_b \right\} + \delta_3 \right] \quad (35)$$

where

$$\begin{aligned} \delta_3 = & 2\delta_1 \left(\frac{1}{15} \frac{R_p^2}{D_a} + \frac{1}{3} \frac{R_p}{k_f} \right) \left[\frac{K_a^2}{k_a} + \frac{1}{15} \frac{(\varepsilon_i + K_a)^2}{1-\varepsilon_a - \varepsilon_b} \left(\frac{r_c^2}{D_i} \right) \right] \\ & + \frac{1-\varepsilon}{\varepsilon} \left[\frac{K_a^3}{k_a^2} + \frac{2}{15} \frac{\varepsilon_i + K_a}{1-\varepsilon_a - \varepsilon_b} \frac{K_a^2}{k_a} \left(\frac{r_c^2}{D_i} \right) + \frac{2}{315} \frac{(\varepsilon_i + K_a)^3}{(1-\varepsilon_a - \varepsilon_b)^2} \left(\frac{r_c^2}{D_i} \right) \right. \\ & \left. + \frac{(\varepsilon_a + \varepsilon_i + K_a)^3}{315} \left\{ 35 \left(\frac{R_p}{k_f} \right)^2 + 14 \left(\frac{R_p^2}{D_a} \right) \left(\frac{R_p}{k_f} \right) + 2 \left(\frac{R_p^2}{D_a} \right)^2 \right\} \right] \end{aligned} \quad (36)$$

4. Two Diffusivity Diffusion Model for Zeolite-type Particles

For beds packed with the zeolite-type particles, many investigators usually choose a model based on the single-phase adsorption instead of two phase adsorption of both gas and adsorbed phases in the microcrystal, due to the strong force field associated with the pore wall. Therefore only the microparticle diffusion equation is replaced by the solid diffusion equation, all the other mass balances being the same.

$$\frac{\partial C_2}{\partial t} = \frac{D_z}{\varepsilon} \frac{\partial^2 C_2}{\partial z^2} - v \frac{\partial C_2}{\partial z} - \frac{3}{R_p} \frac{1-\varepsilon}{\varepsilon} D_a \frac{\partial C_a}{\partial R} \Big|_{R=R_p} \quad (37)$$

$$\frac{\partial C_a}{\partial t} = \frac{D_a}{\varepsilon_a} \frac{1}{R^2} \frac{\partial}{\partial R} \left(R^2 \frac{\partial C_a}{\partial R} \right) - \frac{3}{r_c} \frac{1-\varepsilon_a - \varepsilon_b}{\varepsilon_a} D_i \frac{\partial q}{\partial r} \Big|_{r=r_c} \quad (38)$$

$$\frac{\partial q}{\partial t} = \frac{D_c}{r^2} \frac{\partial}{\partial r} \left(r^2 \frac{\partial q}{\partial r} \right) \quad (39)$$

where the adsorbed phase concentration, q is based upon the microcrystal volume. Hsu and Haynes [1981] formulated a similar model taking into account both a finite rate of adsorption and size distribution of microcrystals. In this derivation, microcrystal size was assumed to be uniform.

Initial and boundary conditions are,

$$C_2(z, 0) = 0, \quad C_a(z, R, 0) = 0, \quad q(z, R, r, 0) = 0 \quad (40)$$

$$C_2(0, t) = \delta(t), \quad C_2(\infty, t) = 0 \quad (41)$$

$$D_a \frac{\partial C_a}{\partial R} \Big|_{R=R_p} = k_f [C_2(z, t) - C_a(z, R_p, t)], \quad \frac{\partial C_a}{\partial R} \Big|_{R=0} = 0 \quad (42)$$

$$\frac{3}{r_c} \cdot D_c \frac{\partial q}{\partial r} \Big|_{r=r_c} = k_c \left[C_a(z, R, t) - \frac{q(z, R, r_c, t)}{K_c} \right], \quad \frac{\partial q}{\partial r} \Big|_{r=0} = 0 \quad (43)$$

Since the microcrystal volume based adsorbed phase concentration, q is related to the particle volume based adsorbed phase concentration, Q by $(1 - \varepsilon_a - \varepsilon_b)q = Q$, linear adsorption rate based upon the microcrystal volume can be changed to the particle volume based adsorption rate by multiplying a factor of $(1 - \varepsilon_a - \varepsilon_b)$.

$$\begin{aligned} \frac{\partial Q}{\partial t} = & (1 - \varepsilon_a - \varepsilon_b) \frac{3}{r_c} \cdot D_c \frac{\partial q}{\partial r} \Big|_{r=r_c} = (1 - \varepsilon_a - \varepsilon_b) k_c \\ & \left[C_a(z, R, t) - \frac{Q(z, R, r_c, t)}{(1 - \varepsilon_a - \varepsilon_b) K_c} \right] \end{aligned} \quad (44)$$

Since $C_i(z, R, r, t) = C_a(z, R, t)$, one can easily obtain the following relationships by comparing the above equation with Eq. (25) at $r = r_c$.

$$k_a = (1 - \varepsilon_a - \varepsilon_b) k_c, \quad K_a = (1 - \varepsilon_a - \varepsilon_b) K_c \quad (45)$$

Hence,

$$\frac{K_a}{k_f} = \frac{K}{k} \tag{46}$$

Furthermore, comparison of the last terms in Eqs. (24) and (38) using $Q=K_a C_i$ and $Q=(1-\epsilon_a-\epsilon_b)q$ results in

$$D_i = K_a \cdot D \tag{47}$$

Considering the relations between the system parameters involved in the two diffusivity and the zeolite-type two diffusivity diffusion models, the two diffusion models are essentially equivalent.

The first absolute moment and variance for the above diffusion model are written respectively as

$$\mu_1' = \frac{L}{v} (1 + \delta_1) \tag{48}$$

$$\mu_2 = 2 \frac{L}{v} \left[\frac{D_i}{\epsilon} \frac{(1 + \delta_1)^2}{v^2} + \delta_a + \delta_b \right] \tag{49}$$

where

$$\delta_1 = \frac{1-\epsilon}{\epsilon} \{ \epsilon_a + (1-\epsilon_a-\epsilon_b)K \} \tag{50}$$

$$\delta_a = \frac{1-\epsilon}{\epsilon} \{ \epsilon_a + (1-\epsilon_a-\epsilon_b)K \}^2 \left(\frac{1}{15} \frac{R_p^2}{D_a} + \frac{1}{3} \frac{R_p}{k_f} \right) \tag{51}$$

$$\delta_b = \frac{1-\epsilon}{\epsilon} (1-\epsilon_a-\epsilon_b)K \left(\frac{K}{k_f} + \frac{1}{15} \frac{r_c^2}{D_c} \right) \tag{52}$$

The third central moment is computed as follows.

$$\mu_3 = 6 \frac{L}{v} \left[2 \frac{D_i}{\epsilon} \frac{1 + \delta_1}{v^2} \left\{ \frac{D_i}{\epsilon} \frac{(1 + \delta_1)^2}{v^2} + \delta_a + \delta_b \right\} + \delta_3 \right] \tag{53}$$

where

$$\begin{aligned} \delta_3 = & 2\delta_1(1-\epsilon_a-\epsilon_b)K_a \left(\frac{1}{15} \frac{R_p^2}{D_a} + \frac{1}{3} \frac{R_p}{k_f} \right) \left(\frac{K_a}{k_f} + \frac{1}{15} \frac{r_c^2}{D_c} \right) \\ & + \frac{1-\epsilon}{\epsilon} \left[(1-\epsilon_a-\epsilon_b)K \left\{ \left(\frac{K_a}{k_f} \right)^2 + \frac{2}{15} \left(\frac{K_a}{k_f} \right) \left(\frac{r_c^2}{D_c} \right) + \frac{2}{315} \left(\frac{r_c^2}{D_c} \right)^2 \right\} \right. \\ & + \frac{\{ \epsilon_a + (1-\epsilon_a-\epsilon_b)K \}^3}{315} \left\{ 35 \left(\frac{R_p}{k_f} \right)^2 + 14 \left(\frac{R_p^2}{D_a} \right) \left(\frac{R_p}{k_f} \right) \right. \\ & \left. \left. + 2 \left(\frac{R_p^2}{D_a} \right)^2 \right\} \right] \end{aligned} \tag{54}$$

RESULTS AND DISCUSSION

1. The First Moment Matching

When all the first absolute moments in various diffusion models are made equal, adsorption equilibrium constants are related in general as listed below.

$$K = \epsilon_p + K_a = \epsilon_a + \epsilon_i + K_a = \epsilon_a + (1-\epsilon_a-\epsilon_b)K \tag{55}$$

The second equality in the middle holds true since the total particle porosity is sum of the macro- and microparticle porosities, i.e., $\epsilon_p = \epsilon_a + \epsilon_i$. In the solid diffusion equation for the zeolite-type particles, microcrystals are considered to be nonporous, i.e., $\epsilon_i = 0$. Hence the last equality holds recovering $K_a = (1-\epsilon_a-\epsilon_b)K$, proved earlier.

2. Variance Matching

By matching both mean and variances from the various diffusion models for the packed bed-type adsorbers, one can easily obtain the following relations between system parameters involved in the model.

$$\begin{aligned} \frac{1}{k} = & \left(\frac{K_a}{\epsilon_p + K_a} \right)^2 \frac{1}{k_a} + \frac{1}{15} \frac{R_p^2}{D_p} + \frac{1}{3} \frac{R_p}{k_f} \\ = & \left(\frac{K_a}{\epsilon_a + \epsilon_i + K_a} \right)^2 \frac{1}{k_a} + \frac{1}{15} \frac{R_p^2}{D_a} + \frac{1}{15} \left(\frac{\epsilon_i + K_a}{\epsilon_a + \epsilon_i + K_a} \right)^2 \frac{r_c^2/D_i}{1-\epsilon_a-\epsilon_b} \\ & + \frac{1}{3} \frac{R_p}{k_f} = \frac{(1-\epsilon_a-\epsilon_b)K_a^2}{\{ \epsilon_a + (1-\epsilon_a-\epsilon_b)K \}^2} \frac{1}{k_a} + \frac{1}{15} \frac{R_p^2}{D_a} \\ & + \frac{1}{15} \frac{(1-\epsilon_a-\epsilon_b)K_a}{\{ \epsilon_a + (1-\epsilon_a-\epsilon_b)K \}^2} \frac{r_c^2}{D_c} + \frac{1}{3} \frac{R_p}{k_f} \end{aligned} \tag{56}$$

In this way the overall effective mass transfer coefficient, k in the LDF model is shown to be related to the system parameters in other diffusion models.

For the relations for the single and two diffusivity diffusion models, the following equality has been obtained.

$$\frac{R_p^2}{D_p} = \frac{R_p^2}{D_a} + \left(\frac{\epsilon_i + K_a}{\epsilon_a + \epsilon_i + K_a} \right)^2 \frac{r_c^2/D_i}{1-\epsilon_a-\epsilon_b} \tag{57}$$

Likewise, matching equations for the single and the zeolite-type two diffusivity diffusion models leads to,

$$\frac{R_p^2}{D_p} = \frac{R_p^2}{D_a} + \frac{(1-\epsilon_a-\epsilon_b)K_a}{\{ \epsilon_a + (1-\epsilon_a-\epsilon_b)K \}^2} \frac{r_c^2}{D_c} \tag{58}$$

Since the various transport rate resistances are additive to the variance for the linear systems, all the external diffusion resistances as well as the internal resistance related to the finite adsorption rate cancel out, leading to the same formula obtained by Kim [1990] which consists of the intraparticle diffusion resistances only.

3. The Third Moment Matching

The third central moments from the LDF, single and two diffusivity, and zeolite-type two diffusivity diffusion models were matched using the relation from the first moment matching to result in the following relationship.

$$\begin{aligned} & 2 \frac{D_i}{\epsilon} \frac{1 + \delta_1}{v^2} \frac{K^2}{k} + \frac{K^3}{k^2} \\ = & 2 \frac{D_i}{\epsilon} \frac{1 + \delta_1}{v^2} \left[\frac{K_a^2}{k_a} + (\epsilon_p + K_a)^2 \left(\frac{1}{15} \frac{R_p^2}{D_p} + \frac{1}{3} \frac{R_p}{k_f} \right) \right. \\ & \left. + 2(\epsilon_p + K_a) \frac{K_a^2}{k_a} \left(\frac{1}{15} \frac{R_p^2}{D_p} + \frac{1}{3} \frac{R_p}{k_f} \right) \right. \\ & \left. + \frac{(\epsilon_p + K_a)^3}{315} \left[35 \left(\frac{R_p}{k_f} \right)^2 + 14 \left(\frac{R_p^2}{D_p} \right) \left(\frac{R_p}{k_f} \right) + 2 \left(\frac{R_p^2}{D_p} \right)^2 \right] + \frac{K_a^3}{k_a^2} \right] \\ = & 2 \frac{D_i}{\epsilon} \frac{1 + \delta_1}{v^2} \left[\frac{K_a^2}{k_a} + (\epsilon_a + \epsilon_i + K_a)^2 \left(\frac{1}{15} \frac{R_p^2}{D_a} + \frac{1}{3} \frac{R_p}{k_f} \right) \right. \\ & \left. + \frac{1}{15} \frac{(\epsilon_i + K_a)^2}{1-\epsilon_a-\epsilon_b} \frac{r_c^2}{D_i} \right] \\ & + 2(\epsilon_a + \epsilon_i + K_a) \left(\frac{K_a^2}{k_a} + \frac{1}{15} \frac{(\epsilon_i + K_a)^2}{1-\epsilon_a-\epsilon_b} \frac{r_c^2}{D_i} \right) \left(\frac{1}{15} \frac{R_p^2}{D_a} + \frac{1}{3} \frac{R_p}{k_f} \right) \\ & + \frac{(\epsilon_a + \epsilon_i + K_a)^3}{315} \left[35 \left(\frac{R_p}{k_f} \right)^2 + 14 \left(\frac{R_p^2}{D_a} \right) \left(\frac{R_p}{k_f} \right) + 2 \left(\frac{R_p^2}{D_a} \right)^2 \right] \\ & + \frac{K_a^3}{k_a^2} + \frac{2}{15} (\epsilon_i + K_a) \left(\frac{K_a^2}{k_a} \right) \left(\frac{r_c^2/D_i}{1-\epsilon_a-\epsilon_b} \right) \\ & + \frac{2}{315} (\epsilon_i + K_a)^3 \left(\frac{r_c^2/D_i}{1-\epsilon_a-\epsilon_b} \right)^2 \\ = & 2 \frac{D_i}{\epsilon} \frac{1 + \delta_1}{v^2} \left[(1-\epsilon_a-\epsilon_b)K \left(\frac{K_a}{k_f} + \frac{1}{15} \frac{r_c^2}{D_c} \right) \right. \\ & \left. + \{ \epsilon_a + (1-\epsilon_a-\epsilon_b)K \}^2 \left(\frac{1}{15} \frac{R_p^2}{D_a} + \frac{1}{3} \frac{R_p}{k_f} \right) \right. \\ & \left. + 2 \{ \epsilon_a + (1-\epsilon_a-\epsilon_b)K \} \right] \end{aligned}$$

$$\begin{aligned}
& (1-\varepsilon_a-\varepsilon_b)K_c \left(\frac{K_c}{k_c} + \frac{1}{15} \frac{r_c^2}{D_c} \right) \left(\frac{1}{15} \frac{R_p^2}{D_a} + \frac{1}{3} \frac{R_p}{k_f} \right) \\
& + \frac{\{\varepsilon_a + (1-\varepsilon_a-\varepsilon_b)K_c\}^3}{315} \left[35 \left(\frac{R_p}{k_f} \right)^2 + 14 \left(\frac{R_p^2}{D_a} \right) \left(\frac{R_p}{k_f} \right) + 2 \left(\frac{R_p^2}{D_a} \right)^2 \right] \\
& + (1-\varepsilon_a-\varepsilon_b)K_c \left[\left(\frac{K_c}{k_c} \right)^2 + \frac{2}{15} \left(\frac{K_c}{k_c} \right) \left(\frac{r_c^2}{D_c} \right) + \frac{2}{315} \left(\frac{r_c^2}{D_c} \right)^2 \right] \quad (59)
\end{aligned}$$

where δ_1 defined below for each diffusion model represents the total relative retention due to both stationary fluid and adsorption inside the particle, compared to that for the nonporous particles with no adsorption.

$$\begin{aligned}
\delta_1 &= \frac{1-\varepsilon}{\varepsilon} K = \frac{1-\varepsilon}{\varepsilon} (\varepsilon_p + K_a) = \frac{1-\varepsilon}{\varepsilon} (\varepsilon_a + \varepsilon_i + K_a) \\
&= \frac{1-\varepsilon}{\varepsilon} \{\varepsilon_a + (1-\varepsilon_a-\varepsilon_b)K_c\} \quad (60)
\end{aligned}$$

Both mean and the third central moments for the single and the two diffusivity diffusion models were matched to result in the following relationship.

$$\begin{aligned}
& \frac{R_p^2}{D_p} \left[\frac{\theta}{Pe} \frac{1+\delta_1}{\varepsilon_p + K_a} + \left(\frac{K_a}{\varepsilon_p + K_a} \right)^2 \frac{1}{k_a} + \frac{1}{21} \frac{R_p^2}{D_p} + \frac{1}{3} \frac{R_p}{k_f} \right] \\
&= \frac{R_p^2}{D_a} \left[\frac{\theta}{Pe} \frac{1+\delta_1}{\varepsilon_a + \varepsilon_i + K_a} + \left(\frac{K_a}{\varepsilon_a + \varepsilon_i + K_a} \right)^2 \frac{1}{k_a} + \frac{1}{21} \frac{R_p^2}{D_a} + \frac{1}{3} \frac{R_p}{k_f} \right] \\
&+ \left(\frac{\varepsilon_i + K_a}{\varepsilon_a + \varepsilon_i + K_a} \right)^3 \frac{r_c^2/D_c}{1-\varepsilon_a-\varepsilon_b} \left[\frac{\theta}{Pe} \frac{1+\delta_1}{\varepsilon_i + K_a} + \left(\frac{K_a}{\varepsilon_i + K_a} \right)^2 \frac{1}{k_a} \right. \\
&+ \left. \frac{\varepsilon_a + \varepsilon_i + K_a}{\varepsilon_i + K_a} \left(\frac{1}{15} \frac{R_p^2}{D_a} + \frac{1}{3} \frac{R_p}{k_f} \right) + \frac{1}{21} \frac{r_c^2/D_c}{1-\varepsilon_a-\varepsilon_b} \right] \quad (61)
\end{aligned}$$

where θ is the space time defined as L/v and Pe , the Peclet number defined as uL/D_p . If both mean and the third central moments from the single and the zeolite-type two diffusivity diffusion models were made equal, one can easily obtain the following relationship.

$$\begin{aligned}
& \frac{R_p^2}{D_p} \left[\frac{\theta}{Pe} \frac{1+\delta_1}{\varepsilon_p + K_a} + \left(\frac{K_a}{\varepsilon_p + K_a} \right)^2 \frac{1}{k_a} + \frac{1}{21} \frac{R_p^2}{D_p} + \frac{1}{3} \frac{R_p}{k_f} \right] \\
&= \frac{R_p^2}{D_a} \left[\frac{\theta}{Pe} \frac{1+\delta_1}{\varepsilon_a + (1-\varepsilon_a-\varepsilon_b)K_c} + \frac{(1-\varepsilon_a-\varepsilon_b)K_c^2}{\{\varepsilon_a + (1-\varepsilon_a-\varepsilon_b)K_c\}^2} \frac{1}{k_c} \right. \\
&+ \left. \frac{1}{21} \frac{R_p^2}{D_a} + \frac{1}{3} \frac{R_p}{k_f} \right] + \frac{(1-\varepsilon_a-\varepsilon_b)K_c^2}{\{\varepsilon_a + (1-\varepsilon_a-\varepsilon_b)K_c\}^3} \frac{r_c^2}{D_c} \left[\frac{\theta}{Pe} \frac{1+\delta_1}{K_c} \right. \\
&+ \left. \frac{1}{k_c} + \frac{\varepsilon_a + (1-\varepsilon_a-\varepsilon_b)K_c}{K_c} \left(\frac{1}{15} \frac{R_p^2}{D_a} + \frac{1}{3} \frac{R_p}{k_f} \right) + \frac{1}{21} \frac{r_c^2/D_c}{K_c} \right] \quad (62)
\end{aligned}$$

Other than the relation obtained by the variance matching, the relations from the third moment matching consist of the cross terms between the transport rate resistances involved, thus becoming more complex compared with the ones from the variance matching.

4. Comparison between Variance and the Third Moment Matching

In order to examine the superiority of the two relationships obtained by either the variance or the third moment matching especially for the cases of the asymmetric response curves, the single and the two diffusivity diffusion models among the four diffusion models considered in this work, were selected for comparison in the time domain. The time domain solutions were computed using the numerical inversion technique of the Laplace transformed solution suggested by Dang and Gibilaro [1974].

First, the two diffusion models were made dimensionless for the sake of comparison efficiency, using the following dimensionless space and time variables.

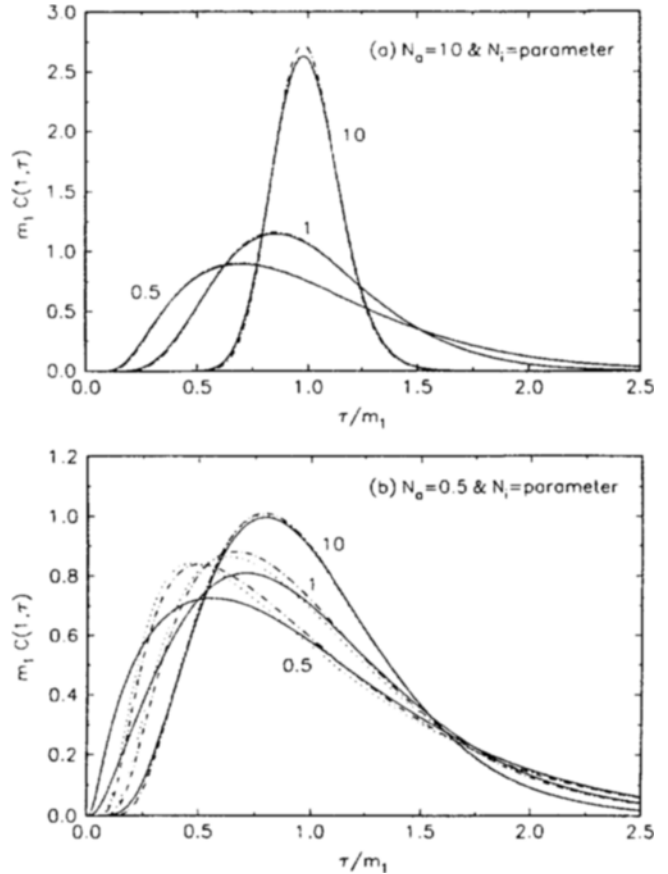


Fig. 1. Time domain elution curves when $\varepsilon=0.4$, $\varepsilon_a=\varepsilon_i=0.3$, $\varepsilon_b=0$, $Pe=1000$, $K_a=200$, $B_a=M_i=B_p=M_p=0$. Solid line, two diffusivity model with N_a and N_i . Dotted line, single diffusivity model with N_p computed from variance matching. Dot dashed line, single diffusivity model with N_p computed from the third moment matching.

$$Z = \frac{z}{L}, \quad \tau = \frac{t}{\theta}, \quad m_1 = \frac{\mu_1'}{\theta} \quad (63)$$

The following dimensionless system parameters were also defined for the single and the two diffusivity diffusion models respectively.

$$N_p = \frac{\theta D_p}{R_p^2}, \quad M_p = \frac{D_p}{k_a R_p^2}, \quad B_p = \frac{D_p}{k_f R_p} \quad (64)$$

$$N_a = \frac{\theta D_a}{R_p^2}, \quad N_i = \frac{\theta D_i}{r_c^2}, \quad M_i = \frac{D_i}{k_a r_c^2}, \quad B_a = \frac{D_a}{k_f R_p} \quad (65)$$

Therefore, the relation from the variance matching between the single and the two diffusivity diffusion models can be rewritten using the dimensionless parameters defined above; for the relation from the variance matching,

$$\frac{1}{N_p} = \frac{1}{N_a} + \frac{1}{1-\varepsilon_a-\varepsilon_b} \left(\frac{\varepsilon_i + K_a}{\varepsilon_i + \varepsilon_i + K_a} \right)^2 \frac{1}{N_i} \quad (66)$$

Likewise, the relation from the third moment matching becomes

$$\frac{1}{N_p} \left[\frac{1+\delta_1}{\varepsilon_p + K_a} \frac{1}{Pe} + \frac{1}{21N_p} \left\{ 1 + 7B_p + 21 \left(\frac{K_a}{\varepsilon_p + K_a} \right)^2 M_p \right\} \right]$$

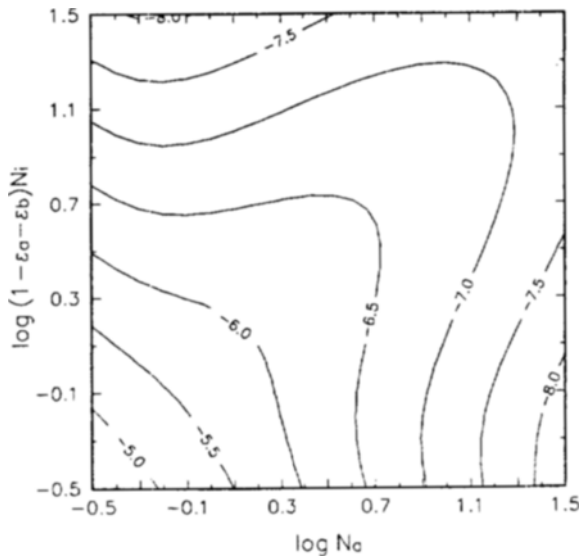


Fig. 2. Contour plot with the single diffusivity parameter N_p from the variance matching. The same parameters as in Fig. 1.

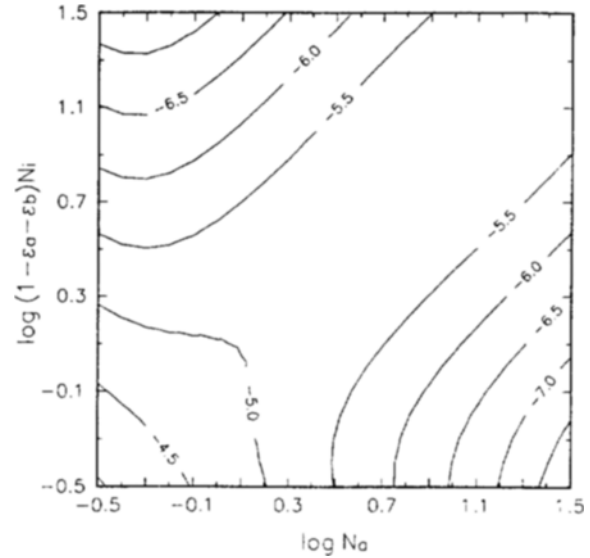


Fig. 3. Contour plot with the single diffusivity parameter N_p from the third moment matching. The same parameters as in Fig. 1.

$$\begin{aligned}
 &= \frac{1}{N_a} \left[\frac{1+\delta_1}{\epsilon_a + \epsilon_i + K_a} \frac{1}{Pe} + \frac{1}{21N_a} (1+7B_a) + \left(\frac{K_a}{\epsilon_a + \epsilon_i + K_a} \right)^2 \frac{M_i}{N_i} \right] \\
 &+ \frac{1}{1-\epsilon_a - \epsilon_b} \left(\frac{\epsilon_i + K_a}{\epsilon_a + \epsilon_i + K_a} \right)^3 \frac{1}{N_i} \left[\frac{1+\delta_1}{\epsilon_i + K_a} \frac{1}{Pe} \right. \\
 &+ \frac{1}{15} \frac{\epsilon_a + \epsilon_i + K_a}{\epsilon_i + K_a} \frac{1+5B_a}{N_a} \\
 &\left. + \frac{1}{21} \frac{1}{1-\epsilon_a - \epsilon_b} \frac{1}{N_i} \left\{ 1 + 21 \left(\frac{K_a}{\epsilon_i + K_a} \right)^2 M_i \right\} \right] \quad (67)
 \end{aligned}$$

Fig. 1 shows the time domain elution curves for the single and two diffusivity diffusion models. The concentration at the bed exit was computed in terms of the dimensionless parameters defined earlier, in addition to the Peclet number, Pe and the adsorption equilibrium constant, K_a . The Peclet number and the adsorption equilibrium constant were chosen as 1000 and 200, respectively. Dimensionless parameters, B_a and B_b were taken as zeroes since the external film mass transfer coefficient is known to be extremely large for the gas phase system. Both M_i and M_b were also taken as zeroes due to the very fast adsorption rate constant for the cases of physical adsorption, although this view is not generally accepted by Smith and his coworkers [Schneider and Smith, 1968; Suzuki and Smith, 1972; Hashimoto and Smith, 1973; Hashimoto and Smith, 1974; Dogu and Smith, 1976]. System parameter N_p for the single diffusivity diffusion model is computed from either Eq. (66) for the variance matching or Eq. (67) for the third moment matching, using N_a and N_i given for the two diffusivity diffusion model. When N_a is rather large (see Fig. 1-a), elution curves from the single diffusivity diffusion model with N_p computed from the variance matching agrees well with those from the two diffusivity diffusion model regardless of the magnitude of N_i . However, elution curves for the single diffusivity diffusion model with N_p computed from the third moment matching deviate a little, and agreement between the two curves gets worse as the curves become symmetric. This point is well expected since N_p is computed from the third moment matching, representing skewness about mean. When N_a is small (Fig. 1-b), the elution curves for the single diffusivity diffusion model with N_p from both variance and the third moment matching deviate much from those

for the two diffusivity diffusion model as N_i gets smaller. When both N_a and N_i are simultaneously small, elution curves emerge shortly after injection and become highly asymmetric. In these extreme circumstances, relation from either variance or the third moment matching is not acceptable. By simulating dynamic adsorbers under plug flow, Kim [1990] has already revealed that the relation from the variance matching does not hold in this region. Other than the expectations that the third moment matching would give better agreement for the cases where both N_a and N_i are very small, the results are unfortunately unsatisfactory.

Both variance and the third moment matching were more thoroughly compared using the contour plot shown in Figs. 2 and 3, respectively. To measure the degree of disagreement, the following sum of error squares were computed.

$$\begin{aligned}
 S(N_a, N_i) &= \sum_{t=1}^{250} [C_2(1, i\Delta\tau; N_a, N_i) - C_1(1, i\Delta\tau; N_p)]^2 \\
 &\text{with } \Delta\tau = 0.01 m_1 \quad (68)
 \end{aligned}$$

In Fig. 2, the single diffusivity parameter, N_p is computed using the variance matching, i.e. Eq. (66), and N_p in Fig. 3 using the third moment matching, Eq. (67). Contour labels were obtained by taking common logarithm of the sum of error squares. Compared to the third moment matching, variance matching gives lower sum of error squares over the whole region of scanning as well as even in the lower lefthand corner where elution curves become highly asymmetric, thus suggesting that the model simplification from the two diffusivity to the single diffusivity diffusion model be done using the variance matching which leads to much simpler formula than the third moment matching.

NOMENCLATURE

- B_a : dimensionless parameter defined in Eq. (65)
- B_b : dimensionless parameter defined in Eq. (64)
- C : adsorbate concentration in the mobile fluid in the LDF model
- C^* : mobile phase concentration in equilibrium with \bar{Q}
- \bar{C} : Laplace transform of C

- C_1 : adsorbate concentration in the mobile fluid in the single diffusivity model
 C_2 : adsorbate concentration in the mobile fluid in the two diffusivity model
 C_m : adsorbate concentration in the macropore
 C_i : adsorbate concentration in the micropore
 C_p : adsorbate concentration in the stationary fluid inside the particle
 D_m : effective macropore diffusivity
 D_s : solid phase diffusivity in the zeolite microcrystal
 D_i : effective micropore diffusivity
 D_p : single effective diffusivity in the particle
 D_e : effective axial dispersion coefficient
 k : overall effective mass transfer coefficient
 K : pseudoadsorption equilibrium constant based on pellet volume
 k_s : adsorption rate constant based on pellet volume
 K_s : adsorption equilibrium constant based on pellet volume
 k_m : adsorption rate constant based on microcrystal volume
 K_m : adsorption equilibrium constant based on microcrystal volume
 k_f : external film mass transfer coefficient (fluid to particle)
 L : length of packed bed
 m_1 : variable defined by μ_1'/θ
 M_1 : dimensionless parameter defined in Eq. (65)
 M_p : dimensionless parameter defined in Eq. (64)
 N_m : dimensionless parameter defined in Eq. (65)
 N_i : dimensionless parameter defined in Eq. (65)
 N_p : dimensionless parameter defined in Eq. (64)
 Pe : Peclet number defined as uL/D_e
 q : adsorbed phase concentration based on the microcrystal volume
 Q : adsorbed phase concentration based on the particle volume
 \bar{Q} : particle volume averaged total adsorbate concentration
 r : radial coordinate of the microparticle
 R : radial coordinate of the particle
 r_p : microparticle radius
 R_p : particle radius
 s : variable in the Laplace transform domain
 t : time
 u : superficial velocity in the empty bed
 v : interstitial velocity in the bed
 z : variable for the axial direction of the bed
 Z : dimensionless variable defined by z/L

Greek Letters

- δ_1 : variable defined in Eq. (60)
 ε : bed porosity
 ε_m : macropore porosity based on the particle volume
 ε_b : volume fraction of binder based on the particle volume
 ε_i : micropore porosity based on the particle volume
 ε_p : total pellet porosity based upon the particle volume
 μ_n' : the n-th absolute moment
 μ_2 : the second central moment or variance
 μ_3 : the third central moment
 θ : space time defined by L/v
 τ : dimensionless time defined by t/θ

REFERENCES

- Dang, N. and Gibilaro, L., "Numerical Inversion of Laplace Transforms by a Simple Curve Fitting Technique", *Chem. Eng. J.*, **8**, 157 (1974).
Dogu, G. and Smith, J. M., "Rate Parameters from Dynamic Experiments with Single Catalyst Pellets", *Chem. Eng. Sci.*, **31**, 123 (1976).
Glueckauf, E. and Coates, J. E., "Theory of Chromatography". *J. Chem. Soc.*, 1315 (1947).
Hashimoto, N. and Smith, J. M., "Macropore Diffusion in Molecular Sieve Pellets by Chromatography", *Ind. Eng. Chem. Fundam.*, **12**(3), 353 (1973).
Hashimoto, N. and Smith, J. M., "Diffusion in Bidisperse Porous Catalyst Pellets", *Ind. Eng. Chem. Fundam.*, **13**(2), 115 (1974).
Hsu, L. K. P. and Haynes, H. W., "Effective Diffusivity by the Gas Chromatography Technique: Analysis and Application to Measurements of Diffusion of Various Hydrocarbons in Zeolite NaY", *AIChE J.*, **27**(1), 81 (1981).
Kim, D. H., "Single Effective Diffusivities for Dynamic Adsorption in Bidisperse Adsorbents", *AIChE J.*, **36**(2), 302 (1990).
Raghavan, N. S. and Ruthven, D. M., "Simulation of Chromatographic Response in Columns Packed with Bidisperse Structured Particles", *Chem. Eng. Sci.*, **40**(5), 699 (1985).
Ruthven, D., "Principles of Adsorption and Adsorption Processes", John Wiley and Sons, New York (1984).
Schneider, P. and Smith, J. M., "Adsorption Rate Constants from Chromatography", *AIChE J.*, **14**(5), 762 (1968).
Suzuki, M. and Smith, J. M., "Dynamics of Diffusion and Adsorption in a Single Catalyst Pellet", *AIChE J.*, **18**(2), 326 (1972).